Naunyn-Schmiedeberg's Arch Pharmacol (2012) 385:861–873
DOI 10.1007/s00210-012-0783-6

ORIGINAL ARTICLE

Evaluation of antibodies directed against human protease-activated receptor-2

Mark N. Adams · Charles N. Pagel · Eleanor J. Mackie · John D. Hooper

Received: 19 March 2012 / Accepted: 13 July 2012 / Published online: 31 July 2012

Abstract Protease-activated receptor 2 (PAR2) is a G protein-coupled receptor activated by intramolecular docking of a tethered ligand that is released by the actions of proteases, mainly of the serine protease family. Here, we evaluate four commercially available anti-PAR2 antibodies, SAM11, C17, N19 and H99, demonstrating marked differences in the ability of these reagents to detect the target receptor in Western blot, immunocytochemical and flow cytometry applications. In Western blot analysis, we evaluated antibody reactivity against both ectopic and endogenous receptors. Against material from transfected cells, we show that SAM11 and N19, and to a lesser extent C17, but not H99, are able to detect ectopic PAR2. Interestingly, these Western blot analyses indicate that N19 and C17 detect conformations of ectopic PAR2 distinct to those recognised by SAM11. Significantly, our data also indicate that Western blot signal detected by SAM11 and C17, and much of the signal detected by N19, against cells endogenously expressing PAR2 is non-specific. Despite confounding non-specific signals, we were able to discern N19 reactivity against endogenous PAR2 as a broad smear that we also observed in ectopically expressing human and mouse cells and that is sensitive to loss of N-glycosylation. In immunocytochemistry analysis, each antibody is able to detect ectopic PAR2 although it appears that H99 detects only a subset of the ectopically expressed receptor. In addition, SAM11 and N19 are able to detect both ectopic and endogenous cell surface PAR2 by flow cytometry. In summary: (1) each antibody can detect ectopic PAR2 by immunocytochemical analysis with SAM11 and N19 suitable for cell surface detection of both ectopic and endogenous receptor by flow cytometry; (2) in Western blot analysis, N19, SAM11 and C17 can detect ectopically expressed PAR2, with only N19 able to detect the endogenous receptor by this technique and (3) in each of these approaches, appropriate controls are essential to ensure that non-specific reactivity is identified.

Keywords Protease-activated receptor-2 · PAR2 · Western blot analysis · Confocal microscopy · Flow cytometry · GPCR

M. N. Adams · J. D. Hooper (✉)
Mater Medical Research Institute,
Aubigny Place, Raymond Terrace, South Brisbane, QLD 4101, Australia
e-mail: jhooper@mmri.mater.org.au

C. N. Pagel · E. J. Mackie
Faculty of Veterinary Science, University of Melbourne,
Parkville, Melbourne, VIC 3010, Australia

Introduction

Discovered in the 1990s, protease-activated receptors (PARs) are a sub-family of G protein-coupled receptor (GPCRs) comprising four members designated PAR1, PAR2, PAR3 and PAR4 (Adams et al. 2011b; Macfarlane et al. 2001; Ramachandran et al. 2012). In contrast to the wider GPCR superfamily, PARs are not activated by binding of a soluble ligand but by proteases that cleave extracellularly within the PAR amino terminus. This mechanism results in irreversible removal of the amino terminal pro-peptide and unmasking of a neoepitope termed the tethered ligand (TL) that binds intramolecularly to induce cellular responses (Macfarlane et al. 2001; Vu et al. 1991). These receptors are almost exclusively activated by trypsin fold serine proteases that have specificity for cleavage after arginine (R) or lysine residues. In particular, PAR1, PAR3 and PAR4 are activated by thrombin, while activation of PAR2 and PAR4 is induced by trypsin (Ishihara et al. 1997; Nystedt et al. 1994; Vu et al. 1991; Xu et al. 1998).

PAR2 consists of 397 amino acids with a predicted molecular weight of 44 kDa and contains seven transmembrane helices, an extracellular amino terminal domain encompassing a signal peptide of 25 residues and a pro-domain of 11 amino acids, three intracellular loops, three extracellular loops and an intracellular carboxy terminal domain of 50

residues. PAR2 also contains consensus motifs for post-translational modifications such as N-glycosylation, ubiquitination, phosphorylation and palmitoylation. Due to the irreversible nature of PAR proteolysis, downstream signal transduction is tightly regulated. Following activation, PAR2 is rapidly uncoupled from downstream signalling by the post-translational modifications phosphorylation and ubiquitination which facilitate interactions with β-arrestin (Jacob et al. 2005; Ricks and Trejo 2009). This scaffolding protein couples PAR2 to the internalisation machinery initiating its desensitisation and trafficking through the early and late endosomes followed by receptor degradation (Adams et al. 2011b).

Human PAR2 is activated by cleavage after R^{36} revealing the TL sequence S^{37}LIGKV (Nystedt et al. 1995). In addition to being activated by trypsin (Nystedt et al. 1994), PAR2 is responsive to mast cell tryptase (Molino et al. 1997), tissue factor (TF)/factor (F)VIIa and TF/FVIIa-generated FXa (Camerer et al. 2000), and kallikrein (KLK) family members KLK2 (Mize et al. 2008), KLK4 (Mize et al. 2008; Ramsay et al. 2008) and KLK5, KLK6 and KLK14 (Oikonomopoulou et al. 2006). From these studies, it is clear that PAR2, unlike the other PARs, functions as a cell surface sensor for a diverse range of extracellular and cell surface-associated proteases. Consistently, PAR2 activation contributes to homeostasis in cardiovascular, respiratory, nervous and musculoskeletal systems, and its dysfunctional signalling is apparent in inappropriate inflammatory responses and several malignancies (Adams et al. 2011b; Georgy et al. 2011, 2010; Lohman et al. 2012; Ramachandran et al. 2012).

Recently, we have evaluated the role of palmitoylation in signalling and trafficking of PAR2 (Adams et al. 2011a). This study was facilitated by use of an anti-PAR2 antibody N19 that we used to evaluate cell surface expression of PAR2 by flow cytometry. Here, we evaluate the ability of the N19 antibody and three other commercially available antibodies, SAM11, H99 and C17, to detect PAR2 by Western blot, confocal microscopy and flow cytometry analysis.

Methods and materials

Reagents Anti-PAR2 antibodies SAM11 (mouse monoclonal; sc-13504), H99 (rabbit polyclonal; sc-5597), C17 (goat polyclonal; sc-8205) and N19 (goat polyclonal; sc-8206) and an anti-caveolin 1 (CAV1; sc-894) antibody were from Santa Cruz Biotechnology (Quantum Scientific Pty Ltd, Murarrie, Australia). An anti-CDCP1 antibody against the last 13 amino acids of this protein was from Abcam (Sapphire Biosciences Pty Ltd., Waterloo, Australia). Anti-FLAG epitope (DYKDDDDK), anti-GAPDH and anti-tubulin antibodies were from Sigma-Aldrich (Castle Hill, Australia). Species-appropriate fluorescently conjugated secondary antibodies suitable for flow cytometry analysis were from Invitrogen (Mulgrave, Australia), and for Western blot analysis, from LiCor (Millennium Science, Surrey Hills, Australia). Precision Plus Protein Dual Color molecular weight standards (#161-0374) were from Bio-Rad Laboratories (Gladesville, Australia).

Expression constructs and cell culture The human PAR2 open reading frame incorporating 3′ sequence encoding a carboxyl terminal FLAG epitope (DYKDDDDK) was amplified by PCR using Expand High Fidelity polymerase mixture (Roche, Castle Hill, Australia) and cloned into the pcDNA3.1neo vector (Invitrogen). A construct encoding PAR2 tagged at the carboxyl terminal with green fluorescent protein (GFP) was described previously (Ramsay et al. 2008). All cell culture media and reagents were from Invitrogen except for fetal calf serum (FCS) (Sigma-Aldrich). Chinese hamster CHO-K1 (CHO) and prostate cancer PC3 and DU145 cell lines were from ATCC (Manassas, VA). CHO cells were grown in DMEM and PC3 and DU145 cells were grown in RPMI1640 medium, each supplemented with 10 % FCS. Lung murine fibroblasts from Par1 null mice (designated NILF) (Andrade-Gordon et al. 1999) expressing human PAR1, PAR2 or PAR4 were from Johnson & Johnson Pharmaceutical Research and Development (Spring House, PA) and cultured in Dulbecco's modified Eagle's medium (DMEM) supplemented with 10 % FCS and 200 μg/ml hygromycin B. All cell lines were cultured in 100 units/ml of penicillin and 100 units/ml of streptomycin in a 5 % CO_2 humidified atmosphere at 37 °C, passaged using 0.5 mM EDTA in phosphate-buffered saline (PBS) and regularly tested for mycoplasma contamination. Transfections were performed using Lipofectamine 2000 according to instructions from the manufacturer (Invitrogen).

Cell lysates, cell fractionations and Western blot analysis Lysates were collected in lysis buffer containing 50 mM Tris (pH 7.4), 150 mM NaCl, 5 mM EDTA, 1 % Triton X-100 (*v*/*v*), 1× protease inhibitor cocktail (Roche), 1 mM sodium vanadate, and 10 mM NaF (lysis buffer). For cell fractionations, cells at 50 % confluence were washed with PBS and distilled H_2O for 30 s to induce hypotonic cell shock. Swollen cells were mechanically resuspended in membrane buffer (5 mM Tris (pH 7.5), 0.5 mM EDTA, 1× protease inhibitor cocktail, 1 mM sodium vanadate, 10 mM NaF) and disrupted by several passes through a 26-gauge needle. Cellular debris was removed by centrifugation (800×*g* for 10 min at 4 °C); then, crude soluble and membrane fractions were collected by ultracentrifugation using a Sorvall MX140 ultracentrifuge with a S100-AT4 rotor (100,000×*g* for 1 h at 4 °C). The supernatant was retained as the crude soluble fraction; then, the pellet containing the crude membrane fraction was resuspended in lysis buffer.

Protein concentration in lysates and crude cell fractions was quantified using a BCA kit (Pierce, Thermo Fisher Scientific, Scoresby, Australia), and these were separated by SDS-PAGE using a 10 % resolving layer and a 4 % stacking layer and transferred to nitrocellulose membranes. After blocking with Odyssey blocking buffer (LiCor), membranes were incubated with primary antibodies overnight at 4 °C, washed with Tris-buffered saline (100 mM Tris, 137 mM NaCl) containing 0.1 % (*v*/*v*) Tween-20 (pH 7.5) (TBS-T) and then incubated with species-appropriate AlexaFluor 680 or IRdye 800-conjugated secondary antibodies for 45 min at ambient temperature. Following washing in TBS-T, membranes were scanned on an Odyssey infrared imaging system (LiCor). The efficiency of protein loading and transfer was assessed by reprobing membranes with an anti-GAPDH antibody. The purity of crude soluble fractions was assessed by reprobing membranes with an anti-tubulin antibody. The purity of crude membrane fractions was assessed with an antibody against either CAV1, a protein embedded in the cytosolic leaflet of cell membranes with both amino and carboxyl termini residing in the cytosol, or the membrane spanning protein CDCP1. Where relevant, signal intensity was determined by densitometry analysis of three independent experiments using Odyssey software (LiCor) with results displayed as mean±SEM relative to values for DU145.

Quantitative real-time PCR PAR2 mRNA expression was assessed by quantitative real-time PCR (qRT-PCR) with reactions performed in 96-well plates (Axygen, Quantum Scientific Pty. Ltd.) containing 2.5 μl diluted cDNA reverse transcribed from total RNA (equivalent to 0.25 μg) in nuclease-free H_2O (1:5), 50 nM forward (CGTCGGGGCTTCCAGGAGGAT) and reverse (TATTGGTTCCTTGGATGGTGCCACTG) primer, 1× final concentration of SYBR green PCR master mix (Applied Biosystems, Scoresby, Australia) and nuclease-free H_2O (total volume of 20 μl). Reactions were performed using an ABI PRISM 7300 real-time PCR system (Applied Biosystems). Cycling conditions were 95 °C for 10 min, 40 cycles of 95 °C for 15 s and 60 °C for 1 min followed by a primer-template dissociation step. Threshold and baseline values were adjusted manually using the ABI PRISM 7300 SDS software (Applied Biosystems). Gene expression was normalised to HPRT1 mRNA levels (forward primer TGAACGTCTTGCTC GAGATGTG; reverse primer CCAGCAGGTCAGCAAA GAATTT) using the comparative CT method (Kaushal et al. 2008).

Confocal microscopy CHO cells seeded onto sterile coverslips were transiently transfected with vector (pEGFP-N1) or PAR2-GFP. After 24 h, cells were washed in PBS, fixed with 2 % formaldehyde, washed and permeabilised with 0.5 % Triton X-100 in PBS for 5 min at room temperature, then blocked for 30 min with 3 % BSA (Sigma-Aldrich) in PBS containing 0.1 % Triton X-100. Incubations with anti-PAR2 antibodies SAM11, H99, C17 and N19 (1:70) were performed in blocking buffer overnight at 4 °C. Cells were then washed with PBS and incubated with species-appropriate AlexaFluor 568 tagged secondary antibodies (1:1,000) in blocking buffer for 1 h at room temperature. Cells were then stained with 4′,6-diamidino-2-phenylindole (DAPI) to visualise nuclei. After a final wash in PBS, coverslips were mounted onto slides using Immuno-Fluore mounting media (MP Biomedicals, Seven Hills, NSW, Australia) and sealed. Immunofluorescence was examined using a Leica SP5 confocal microscope (Leica Microsystems, Gladesville, Australia). Image series through the Z axis of cells within fields of interest were acquired. For consistency of analysis, displayed images are of Z planes that include cell nuclei as evidenced by staining with the DNA intercalating agent DAPI. Images were processed using MetaMorph software and displayed using Corel Draw ×5.

Flow cytometry Adherent cells at 50 % confluence were lifted non-enzymatically and counted, and 2.5×10^5 cells washed and stained with mouse anti-PAR2 antibody SAM11 or goat anti-PAR2 antibody N19 (2 μg/1×10^6 cells) in PBS containing 2 % FCS for 30 min at 4 °C. In some experiments, before antibody staining, to remove cell surface PAR2, resuspended cells were treated with 50 nM trypsin for 15 min at 37 °C. After washing with PBS, cells were stained with an AlexaFluor 488-conjugated secondary antibody, and 20,000 events were collected and analysed on a Beckman Coulter FC500 flow cytometer. For all experiments, mean fluorescence intensity (MFI) values were calculated by subtracting secondary only staining from specific anti-PAR2 staining.

Results

Anti-PAR2 antibodies SAM11, C17 and N19 but not H99 detect ectopically expressed PAR2 by Western blot analysis

We first evaluated the ability of the four anti-PAR2 antibodies, SAM11, C17, N19 and H99, to detect PAR2 by Western blot analysis. As shown in Fig. 1a, these antibodies were generated against four distinct domains of human PAR2; mouse monoclonal antibody SAM11 was generated against residues 37–50 which are located immediately following the activation site of PAR2, goat polyclonal antibody C17 against unspecified residues within the PAR2 carboxyl terminal, goat polyclonal antibody N19 against unspecified residues within the amino terminal of activated PAR2 and rabbit polyclonal antibody H99 was generated against peptide spanning residues 230–328 of PAR2. It is important to note that the amino acid sequence targets of two of the antibodies, N19 and C17, are not available from the supplier, and that the epitope recognised by antibody H99 has not been specifically mapped

within the 99 residues of the peptide used for immunizations. For Western blot analyses, CHO cells were transiently transfected with vector or an expression construct encoding PAR2 tagged at the carboxyl terminal with a Flag epitope. Lysates were probed with the four anti-PAR2 antibodies as well as an anti-Flag antibody. As shown in Fig. 1b, the anti-Flag antibody exclusively detected bands in lysates from CHO cells transfected with the PAR2-Flag expression construct. This antibody detected PAR2 predominantly as bands centred at ~75 and ~130 kDa (Fig. 1b, right panel short exposure). However, longer exposure detected this protein as a smear from ~60 to ~250 kD with fainter protein laddering from ~30 to 60 kDa (Fig. 1b, right panel long exposure). Each of the other antibodies, except H99, also detected bands that were specific to lysates from CHO cells transfected with the PAR2-Flag expression construct. Interestingly, whereas SAM11 and anti-Flag signals were very similar, signal detected by C17 and N19 appeared as a smear from ~30 to ~250 kD, reminiscent of signal previously reported by us for anti-Myc Western blot analysis of lysates from CHO cells transiently transfected with a PAR2-Myc expression construct (Adams et al. 2011a). These observations may indicate that epitopes recognised by SAM11 and the anti-Flag antibody are masked in PAR2-Flag conformations that migrate from ~30 to 60 kDa. In addition, although these results indicate that SAM11, C17 and N19 are able to detect ectopically expressed PAR2, each antibody showed some level of cross-reactivity with non-specific bands from vector-transfected cells. SAM11 exhibited minor cross-reactivity with a band of ~75 kDa that was also detected in lysates from vector-transfected cells, C17 with non-specific bands at ~70, ~100 and ~150 kDa, and N19 with non-specific bands faintly apparent at ~50 and ~200 kDa. Anti-GAPDH antibody Western blot analysis indicated that approximately equal amounts of lysate were present in each lane (a panel representative of each membrane is shown below the SAM11 data in Fig. 1b).

To increase the likelihood of distinguishing specific from non-specific antibody reactivity, based on the observation that PAR2 is an integral membrane protein with seven membrane spanning domains, we performed Western blot analysis on crude membrane and soluble fractions from CHO cells transiently transfected with vector or our PAR2-Flag expression construct. The purity of membrane fractions was assessed by Western blot analysis using an antibody that detects CAV1, a protein embedded in the cytosolic leaflet of cell membranes with both amino and carboxyl termini residing in the cytosol. As shown in Fig. 1c, as was seen in whole cell lysates, shorter exposures revealed that the anti-Flag antibody and SAM11 detected bands centred at ~75 and ~130 kDa (Fig. 1c, right panel) in the membrane fraction from CHO cells transfected with the PAR2-Flag expression construct (Fig. 1c). Also consistent with analysis of whole cell lysates, longer exposures revealed PAR2 in the membrane fraction as a smear from ~60 to ~250 kD with fainter protein laddering from ~30–60 kDa (data not shown). C17 and N19 also detected protein that was exclusively present in the membrane fraction from PAR2-Flag-transfected CHO cells, and as was seen with analysis of whole cell lysates, these antibodies detected PAR2-Flag as a smear from ~30 to ~250 kD (Fig. 1b and c). C17 and N19 also detected high molecular weight bands in soluble fractions which were non-specific as these were also apparent in soluble fractions from vector-transfected cells (Fig. 1c). Consistent with Western blot analysis of whole cell lysates (Fig. 1b), H99 did not detect any bands specific to the membrane fraction of PAR2-Flag-expressing cells (Fig. 1c). Importantly, anti-CAV1 Western blot analysis showed no contamination of soluble proteins with membrane fractions, further suggesting that the signals detected in soluble fractions by C17 and N19 are non-specific. These results indicate that anti-PAR2 antibodies SAM11, C17 and N19 are capable of detecting ectopically expressed PAR2. However, it is important to note that appropriate controls, such as material from vector-transfected cells and cell fractionation, are required to identify those signals due to specific reaction with PAR2 epitopes.

Anti-PAR2 antibodies SAM11, C17 and N19 detect ectopically expressed PAR2 by immunocytochemical analysis

We next assessed the ability of the four antibodies to detect PAR2 by immunocytochemical analysis. For this approach, CHO cells were transiently transfected with an expression construct encoding PAR2 tagged at the carboxyl terminal with GFP (Ramsay et al. 2008). Importantly, the GFP tag does not affect PAR2 signalling or receptor trafficking, allowing detection of ectopically expressed PAR2 that localises to similar cellular compartments as the endogenous receptor (Dery et al. 1999; Roosterman et al. 2003). Transfected cells were fixed, permeabilized and stained with anti-PAR2 antibodies followed by fluorescently conjugated species-appropriate secondary antibodies. Stained cells were imaged by confocal microscopy to examine the extent of overlap between PAR2-GFP signal (green) and the signal detected by the anti-PAR2 antibodies (red), with the overlapping signal apparent as yellow in merged

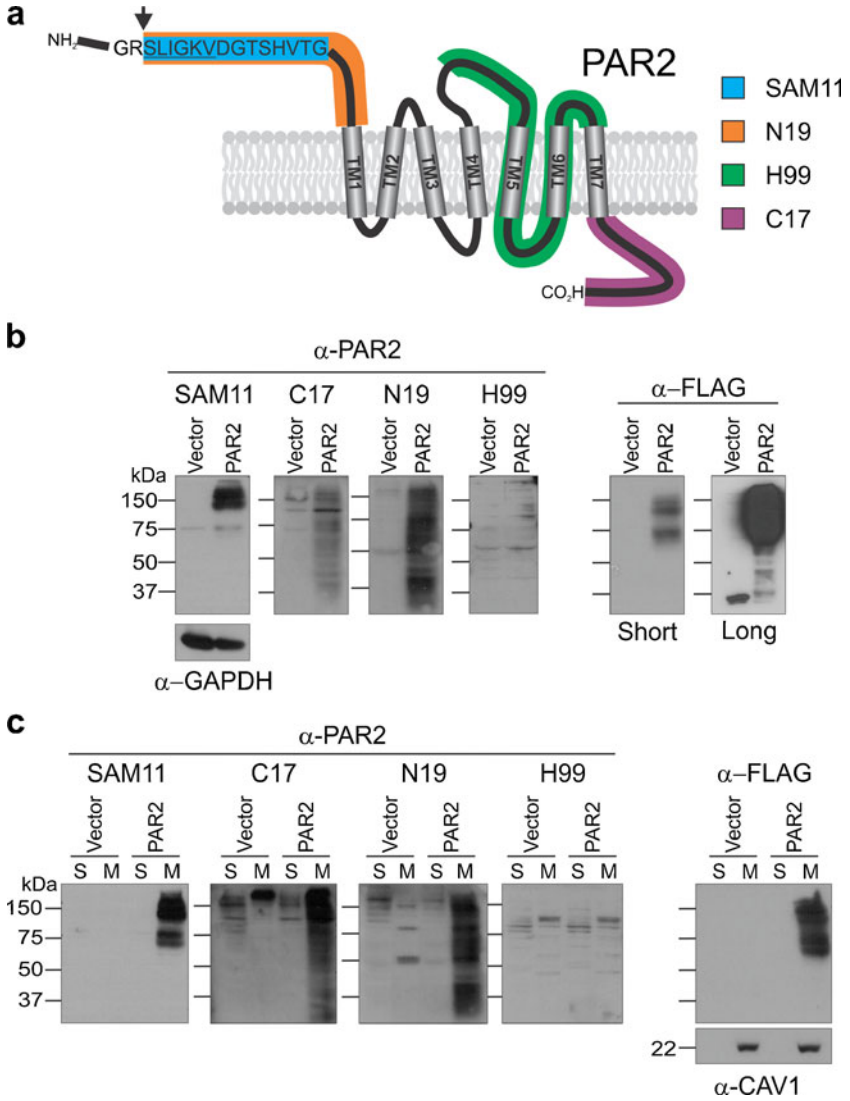

Fig. 1 **a** Schematic representation of the structure of human PAR2 including epitopes for the anti-PAR2 antibodies SAM11 (*blue*), N19 (*orange*), H99 (*green*) and C17 (*purple*). The *arrow* shows the cleavage sites for removal of the receptor activation pro-peptide to yield the TL sequence SLIGKV of human PAR2 (*underlined*). **b** Western blot analysis of lysates from CHO cells transiently transfected with vector or a PAR2-Flag expression construct probed with anti-PAR2 antibodies SAM11, C17, N19 and H99 (1:100) and anti-Flag (1:5,000) and anti-GAPDH antibodies (1:10,000). The data are representative of three independent experiments. Short and long exposures are shown for the anti-Flag analysis. The anti-GAPDH panel is representative of the loading control for each blot. **c** Western blot analysis of soluble (*S*) and membrane (*M*) fractions from CHO cells transiently transfected with vector or a PAR2-Flag expression construct probed with anti-PAR2 antibodies SAM11, C17, N19 and H99 (1:100), and an anti-FLAG antibody (1:5,000). As each panel analysed material from the same cell fractions, the anti-CAV1 (1:1,000) panel is representative of the level of contamination of soluble fractions. All data are representative of three independent experiments

images. Image series were acquired from the apex to the basement of cells, and the Z planes shown in Fig. 2 bisect cell nuclei as evidenced by staining with the DNA intercalating agent DAPI. As shown in Fig. 2, PAR2-GFP signal was apparent throughout the cytoplasm of cells up to the plasma membrane boundary but was not observed in cell nuclei (second column). These images were reminiscent of staining reported previously by us of CHO cells expressing PAR2-mCherry and PAR2-GFP (Adams et al. 2011a). PAR2-GFP signal overlapped closely with staining from antibodies SAM11 (third column, top row), C17 (third column, third row) and N19 (third column, fourth row). Importantly, for each of the four antibodies, a signal was not apparent from cells not expressing PAR2-GFP, which are apparent as DAPI-stained nuclei in Fig. 2 (first column), indicating that these reagents were not reacting non-specifically with proteins expressed endogenously by CHO cells. Interestingly, H99 staining was restricted to peri-nuclear and distinct

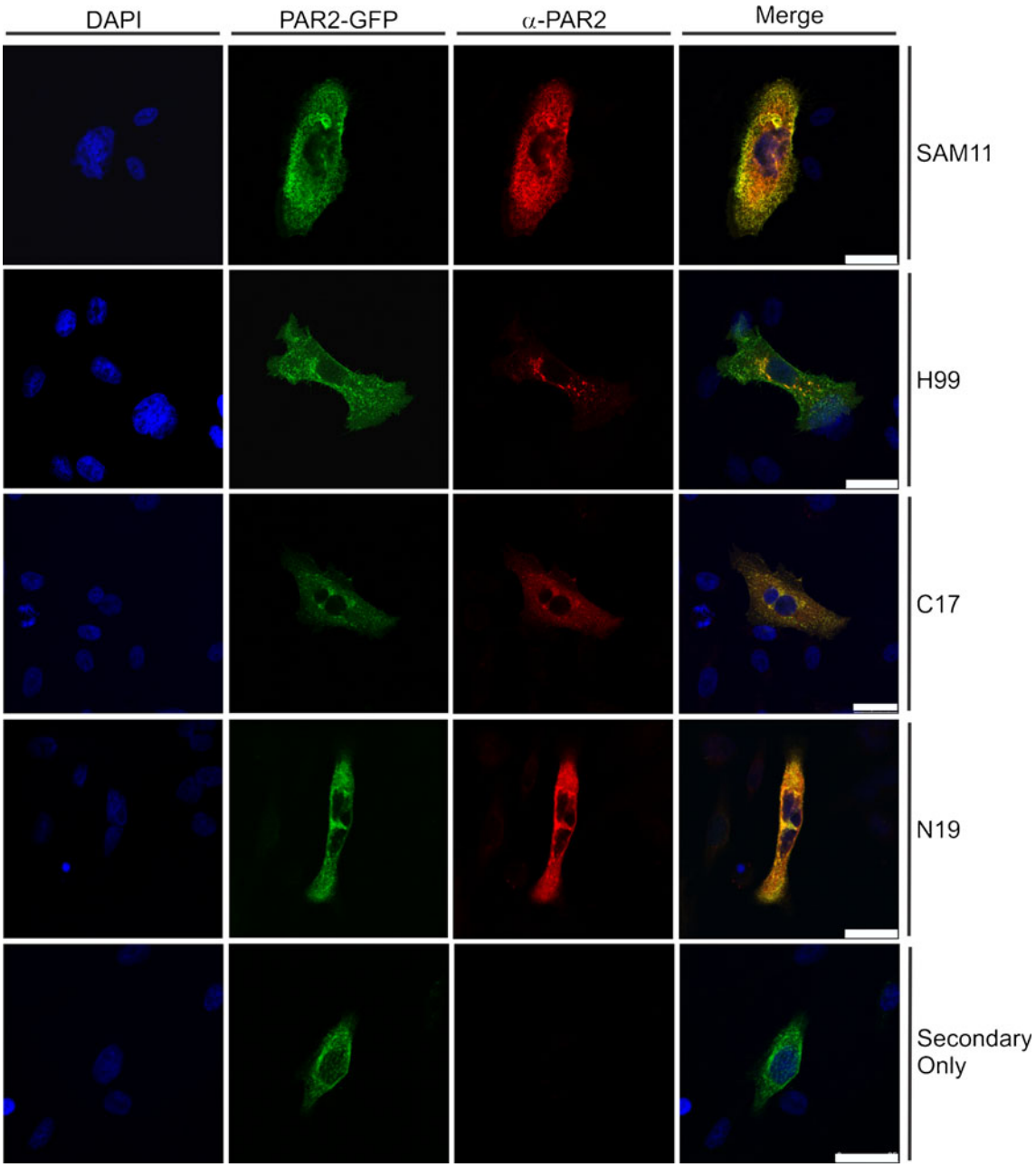

Fig. 2 Confocal microscopy analysis of CHO cells transiently transfected with a PAR2-GFP expression construct and stained with DAPI (*blue*) to visualise cell nuclei as well as the indicated anti-PAR2 antibody (1:70) followed by species-appropriate fluorescently conjugated secondary antibodies (α-PAR2, red; 1:1,000). PAR2-GFP signal (*green*) overlayed on signal from anti-PAR2 antibody (*red*) is shown in merged images (*yellow*). In these merged images, the lack of antibody reactivity against cells not expressing PAR2-GFP (cells stained only with DAPI (*blue*)) demonstrates that SAM11, H99, C17 and N19 had no non-specific cross-reactivity with CHO cell proteins. The "*Secondary Only*" row shows signal from cells stained only with fluorescently conjugated anti-mouse secondary antibody (data from anti-rabbit and anti-goat secondary antibodies were also clear of non-specific signal). *Scale bars*, 25 μm. Images are representative of data from four independent experiments

cytoplasmic structures that only partially overlapped the PAR2-GFP signal (third column, second row). Controls in which only secondary antibodies were incubated with cells were clear of staining (the anti-mouse secondary is shown in the bottom row; data for anti-rabbit and anti-goat secondary antibodies are not shown). These data indicate that in immunocytochemical applications, the antibodies SAM11, C17 and N19 are capable of detecting ectopically expressed PAR2. In addition, it is possible that H99 is also able to detect a subset of ectopically expressed PAR2 in this application; however, this requires further evaluation.

Evaluation of the specificity of anti-PAR2 antibodies against endogenous receptor in Western blot analysis

We next assessed the ability of SAM11, C17 and N19 to detect endogenous PAR2 by Western blot analysis. Antibody H99 was excluded from this analysis because it was incapable of detecting ectopic PAR2 by this technique (Fig. 1). Analysis was performed on prostate cancer PC3 and DU145 cells which have previously been shown to express this receptor (Mize et al. 2008; Ramsay et al. 2008), and our qRT-PCR analysis showed that PAR2 mRNA levels in PC3 cells are ~4-fold higher than in DU145 cells (Fig. 3a). As for examination of ectopic PAR2, Western blot analysis for endogenous receptor was performed on cellular material separated into soluble and membrane fractions. As shown in

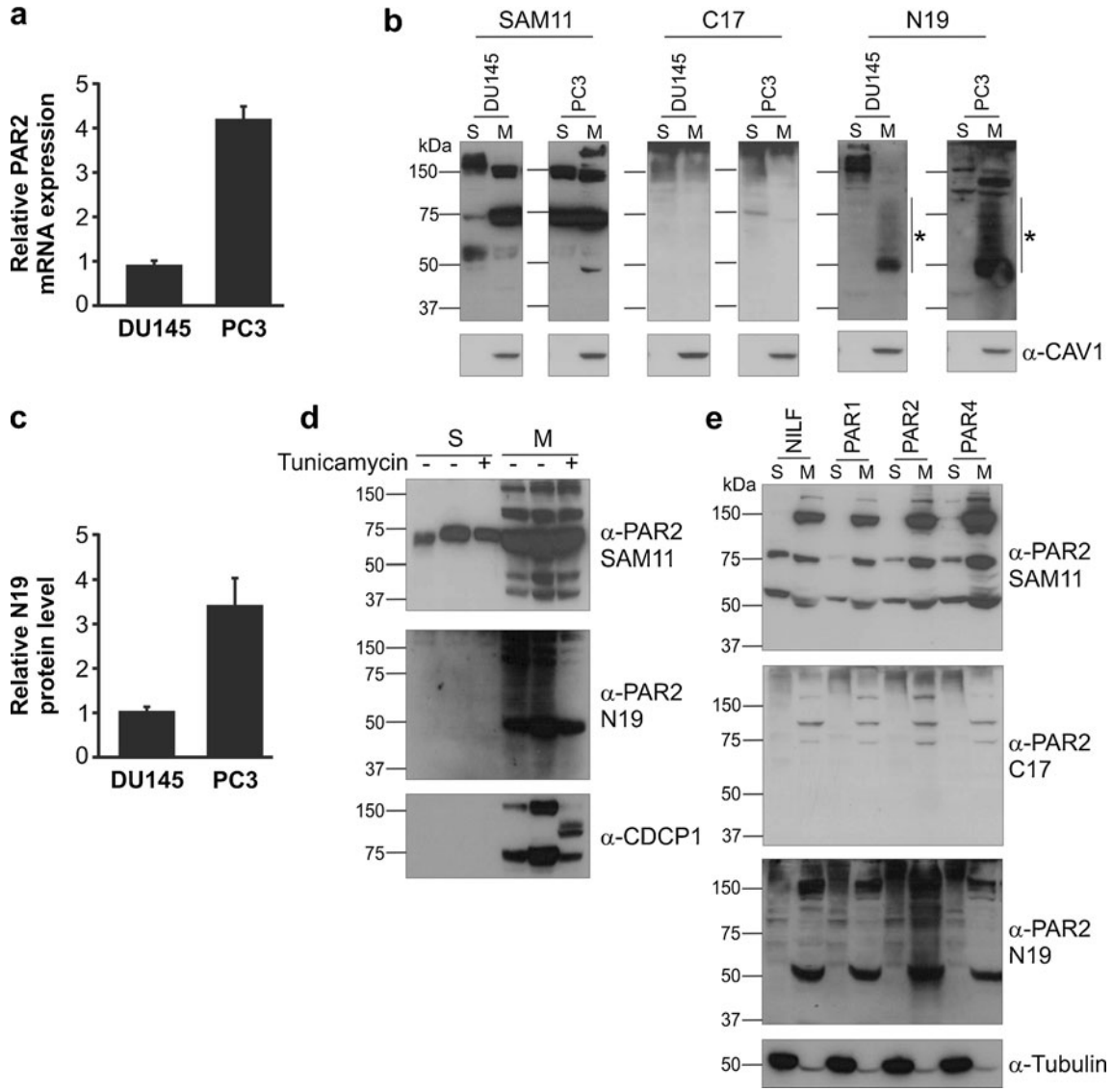

Fig. 3 **a** Graphical representation of PAR2 mRNA expression in prostate cancer PC3 and DU145 cell lines determined by qRT-PCR analysis. Comparative CT values normalised to the housekeeping gene HPRT1 are presented as average fold expression relative to expression in DU145 cells. Values were calculated from three independent experiments performed in triplicate and are shown as mean±SEM. **b** Western blot analysis of soluble and membrane fractions from DU145 and PC3 cells probed with anti-PAR2 antibodies SAM11, C17 and N19 (1:100), and an anti-CAV1 antibody (1:1,000). *membrane fraction-specific smear. *S* soluble fraction, *M* membrane fraction. **c** Graphical representation of densitometry analysis of data from anti-PAR2 N19 antibody Western blot analysis comparing membrane fraction-specific protein expression in PC3 and DU145 cells. The membrane fraction-specific smear highlighted by an *asterisk* were analysed by densitometry with values determined from three independent experiments and are displayed as ±SEM. **d** Anti-PAR2 N19 (α-PAR2; 1:100) and anti-CDCP1 (1:1,000) Western blot analysis of soluble (*S*) and membrane (*M*) fractions from PC3 cells untreated (−) or treated (+) with the N-glycosylation inhibitor tunicamycin. The data are representative of three independent experiments. **e** SAM11, C17 and N19 (1:100), and anti-tubulin (1:5,000) Western blot analysis of soluble (*S*) and membrane (*M*) fractions from mouse fibroblasts from PAR1 knockout mice (NILF) and NILF cells stably expressing human PAR1, PAR2 or PAR4

Fig. 3b, this analysis indicated that antibody N19 detected a membrane fraction-specific smear from ~50 to greater than ~150 kDa, including a predominant band of ~50 kDa, in both cell types (see asterisk in Fig. 3b). In contrast, the predominant signals detected with antibody SAM11 were present in both fractions, although two membrane-specific bands were apparent in PC3 fractions at ~45 and ~250 kDa. Of note, bands detected by antibody C17 were present in both membrane and soluble fractions suggesting that this antibody is not able to detect endogenous PAR2. Densitometric analysis of the membrane fraction-specific smear recognised by antibody N19 indicated that the levels of protein detected by this antibody in PC3 and DU145 cells were consistent with PAR2 mRNA levels in these cells (compare Fig. 3a and c). To further examine the ability of SAM11 and N19 to detect endogenous PAR2, we performed Western blot analysis on soluble and membrane fractions from untreated and tunicamycin-treated PC3 cells. Tunicamycin inhibits the addition of N-linked glycans to proteins. As a control to assess the efficiency of tunicamycin treatment, we also examined its effect on the molecular weight of the integral membrane protein CDCP1 (Wortmann et al. 2009) which is known to contain 30–40 kDa of N-linked glycans (Hooper et al. 2003). As shown in Fig. 3d (top panel), tunicamycin inhibition of N-glycosylation had no effect on the bands detected by antibody SAM11 in soluble and membrane fractions. Noteworthy from the analysis shown in Fig. 3d is an additional band at ~110 kDa that was sometimes apparent when we analysed for an endogenous receptor. It is also worth noting that in some analyses of these fractions, all bands except the ~75-kDa band were observed only in the membrane fraction. Whether these membrane-specific and tunicamycin-resistant bands represent endogenous PAR2 requires further investigation. In contrast with SAM11 analysis, the membrane-specific smear detected by antibody N19 collapsed to a band of ~50 kDa on inhibition of N-glycosylation (Fig. 3d, middle panel). Evidence that tunicamycin was effective at inhibiting N-glycosylation was apparent from the reduction in the molecular weight of 135 kDa CDCP1 expressed by PC3 cells (He et al. 2010) to bands of 95–105 kDa (Fig. 3d, bottom panel).

To further evaluate the reactivity of SAM11, C17 and N19 in Western blot analysis, we examined soluble and membrane fractions from cells from Par1 knockout mice (referred to as NILF cells) stably expressing human PAR1, PAR2 or PAR4. Whereas these lines have been available for over a decade (Andrade-Gordon et al. 1999), it was not possible to perform experiments using cells isolated from Par2 knockout mice as these have not been reported. Importantly, it is known that these NILF-PAR cell lines express the respective family member as we have previously shown that each responds to receptor selective agonists (Ramsay et al. 2008). As shown in Fig. 3e, despite three repetitions of these assays, reactivity of SAM11 and C17 was similar against material from NILF, NILF-PAR1, NILF-PAR2 and NILF-PAR4 cells. In addition, despite high-stringency wash conditions, N19 Western blot analysis of these mouse-derived cell lines produced a much higher background than analysis of transfected hamster cell lines (Fig. 1b and c) or endogenous expressing human cell lines (Fig. 3b and d). Despite this background, it is apparent that antibody N19 showed the highest reactivity against a protein smear from ~30 to ~250 kDa in the membrane fraction from NILF-PAR2 cells (Fig. 3e). In contrast, this signal was not seen in the membrane fraction from the other lines. We consider that it is likely that this smear represents reactivity against ectopically expressed PAR2 as a similar N19-reactive smear was observed in both transiently transfected CHO cells (Fig. 1b and c) and endogenously expressing PC3 and DU145 cells (Fig. 3b and d). It is also noteworthy that antibody N19 strongly detected defined bands at ~50 and ~150 kDa in the membrane fraction of all four cell lines. Although this may indicate non-specific binding, it is also possible that these bands are due to the presence of mouse Par2. In addition, this antibody exhibited lower levels of reactivity against a protein smear from ~60 kDa to greater than ~250 kDa in the soluble fraction of each cell line. It is possible that this is due to the presence of a small amount of contamination of this fraction by membrane proteins.

Anti-PAR2 antibodies SAM11 and N19 detect ectopic and endogenous PAR2 by flow cytometry analysis

We have recently examined the ability of antibodies SAM11 and N19 to detect cell surface PAR2 by live cell flow cytometry analysis (Adams et al. 2011a). These antibodies were chosen as each was generated against extracellular PAR2 epitopes that are located carboxyl terminal to the receptor activation site (Fig. 1a), thereby permitting the detection of nascent and activated receptors. Our data indicated that both SAM11 and N19 were capable of detecting cell surface PAR2 ectopically expressed by CHO cells as well as the receptor endogenously expressed by PC3 cells. Of note, the N19 signal was stronger than the SAM11 signal in both cell types, suggesting that N19 is the more sensitive antibody in flow cytometry applications. To further evaluate the specificity of these antibodies, we performed a series of experiments on cells that had been treated with trypsin. As this protease activates PAR2 and induces its rapid internalisation (Bohm et al. 1996; Ricks and Trejo 2009), trypsin treatment should result in reduced cell surface binding of antibodies that specifically detect this receptor. CHO-PAR2 and PC3 cells were lifted non-enzymatically, and untreated

and trypsin-treated cells (50 nM for 5 min 37 °C) were stained with SAM11 or N19 and subjected to flow cytometry analysis. As shown in Fig. 4a, trypsin treatment caused a reduction in fluorescence detected by SAM11 from both CHO-PAR2 (left panel; MFI 44.2±3.4 reduced to 34.7±1.9) and PC3 (right panel; MFI 15.7±2.3 reduced to 8.4±0.7) cells. Similarly, as shown in Fig. 4b, trypsin treatment also caused a reduction in fluorescence detected with antibody N19 from both CHO-PAR2 (left panel; MFI 48.6±0.7 reduced to 9.13±1.8) and PC3 (right panel; MFI 26.8±2.1 reduced to 7.4±0.8) cells. In control experiments, untreated and trypsin-treated vector-transfected CHO cells showed MFI values of <2.3 with each antibody and analysis with only secondary antibody MFI values of <1.0 (Fig. 4, legend). These data indicate that SAM11 and N19 both specifically detect ectopic and endogenous cell surface PAR2 by flow cytometry confirming the robustness of these reagents in this application.

Discussion

To facilitate studies to examine the role of the protease-activated GPCR PAR2 in physiological and disease settings, we have evaluated four commercially available anti-PAR2 antibodies, SAM11, C17, N19 and H99. In summary, our data highlight marked differences in the ability of these reagents to detect the target receptor in Western blot, immunocytochemical and flow cytometry applications and demonstrate the need for careful selection of appropriate controls to identify PAR2-specific reactivity in each of these approaches.

We demonstrate that antibody N19 has the most utility, detecting ectopic and endogenous PAR2 as a broad smear in Western blot analysis. However, it is important to note that N19 shows non-specific reactivity in this application that we found particularly evident when analysing for endogenous receptor and cautions against using this antibody to detect endogenous PAR2 unless appropriate controls are available. In our hands, the identification of specific PAR2 reactivity was facilitated by examining cellular material separated into soluble and membrane fractions and by analysis of material from cells in which N-glycosylation was inhibited, as well as comparison of material from mouse Par1-/- fibroblasts stably expressing human PAR1, PAR2 or PAR4. We also suggest that other controls could include analysis of fractions from cells silenced for PAR2 expression and cells from PAR2 knockout mice. Our results also indicate that N19 detects ectopic PAR2 in immunocytochemical applications showing a lack of cross-reactivity with endogenous host cell

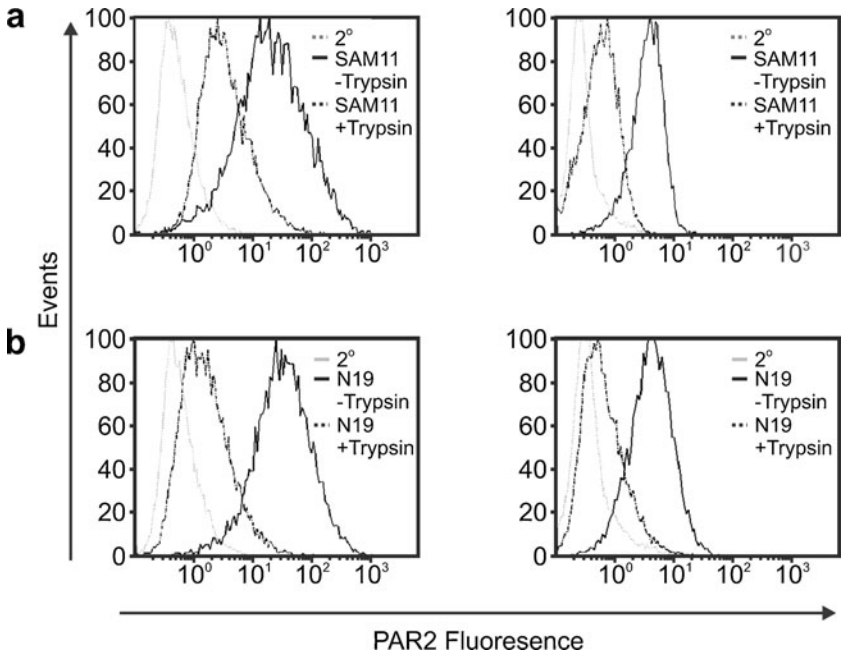

Fig. 4 **a** Antibody SAM11 flow cytometry analysis of non-permeabilised CHO-PAR2 (*left*) and PC3 (*right*) cells either untreated (−*Trypsin*) or treated (+*Trypsin*) with trypsin (50 nM) for 15 min at 37 °C. MFI values: untreated CHO-vector cells, 1.92±0.7; treated CHO-vector cells, 1.87±0.8; untreated CHO-PAR2 cells, 44.2±3.4; treated CHO-PAR2 cells, 34.7±1.9; untreated PC3 cells, 15.7±2.3; treated PC3 cells, 8.4±0.7; secondary antibody only <1.0. **b** Antibody N19 flow cytometry analysis of non-permeabilised CHO cells transiently transfected with a PAR2-Flag expression construct (*left*) and PC3 (*right*) cells either untreated (−*Trypsin*) or treated (+*Trypsin*) with trypsin (50 nM) for 15 min at 37 °C. MFI values: untreated CHO-vector cells, 2.12±0.6; treated CHO-vector cells, 2.23±0.7; untreated CHO-PAR2 cells, 48.6±0.7; treated CHO-PAR2 cells, 9.13±1.8; untreated PC3 cells, 26.8±2.1; treated PC3 cells 7.4±0.8; secondary antibody only <1.0. Data in each panel are representative of three independent experiments

proteins. In addition, N19 is able to detect ectopically expressed and endogenous receptor in flow cytometry analysis.

It is also clear from our analyses that SAM11 is able to detect ectopically expressed PAR2 in Western blot and immunocytochemical approaches and both ectopic and endogenous receptor by flow cytometry. However, it is not yet clear whether this antibody is able to detect endogenous PAR2 by Western blot analysis. Despite performing this analysis on many occasions, we were not able to obtain consistent data on the specificity of SAM11 for endogenous PAR2. An indication that this antibody can detect endogenous PAR2 came from our observation that the banding pattern observed in the membrane fraction from ectopically expressing cells (Fig. 1c) corresponded with the most prominent bands (centred at ~75 and ~130 kDa) seen by us for endogenous receptor in DU145 and PC3 prostate cancer cells (Fig. 3b). However, on some occasions, these bands were also seen in soluble fractions that were clear of the membrane markers CAV1 and CDCP1 (compare Fig. 3b and d) potentially indicating that these represent non-specific binding. Also arguing against the specificity of SAM11 for endogenous PAR2 in Western blot analysis were data showing that SAM11 reactivity is unaffected by inhibition of N-glycosylation (Fig. 3d) and the lack of selectivity we observed for this antibody for PAR2 over PAR1 and PAR4 (Fig. 3e). In addition, Kagota and colleagues have recently reported that SAM11 shows the same reactivity to arterial tissue from wildtype and Par2 null mice (Kagota et al. 2011). While on balance it would appear that SAM11 is not suitable for Western blot analysis of endogenous PAR2, we propose that further experimentation is required before this conclusion can be made definitively. This analysis will also likely be facilitated by examination of fractions from cells silenced for PAR2 expression and cells from PAR2 knockout mice.

Antibody C17 was also able to detect ectopically expressed PAR2 by Western blot (although less efficiently than N19 and SAM11) and immunocytochemistry analysis, but there was no evidence that it detects endogenous receptor by Western blot approaches. Antibody H99 demonstrated the least utility of any of the four examined antibodies showing a complete lack of specific PAR2 reactivity by Western blot analysis and limited reactivity against ectopically expressed receptor in immunocytochemical analysis. Whereas each of the other antibodies showed a high level of specificity against ectopic PAR2 by immunocytochemistry, it appears that H99 may detect only intracellular, including peri-nuclear-located, ectopic PAR2. Although this requires further evaluation, it is possible that the H99 epitope is masked during certain stages of cellular processing. In this regard, the selective detection of PAR2 within peri-nuclear cellular compartments such as the endoplasmic reticulum or Golgi apparatus during secretory trafficking may have experimental benefit. Although we have shown that SAM11, C17 and N19 efficiently detect ectopic PAR2 by immunocytochemical analysis while H99 appears to detect a subset of the expressed receptor, additional experiments are required to observe if any of these four antibodies are capable of detecting the endogenous receptor.

A noteworthy and somewhat perplexing finding from this study is the difference in banding patterns detected by the antibodies that we observed as having some level of specific reactivity against ectopically expressed PAR2 in Western blot analysis (SAM11, C17 and N19). This is highlighted most obviously in Fig. 1c which showed that whereas N19 and C17 detect ectopic PAR2 as broad smears from ~30 to ~250 kDa, and spanning the predicted molecular weight (44 kDa), SAM11 detects it largely as defined bands centred at ~75 and ~130 kDa. It is important to highlight that for each antibody, PAR2 reactive bands were identified by excluding bands that were also observed in fractions from vector-transfected cells or in the soluble fraction of PAR2-Flag-transfected cells. The specificity of the SAM11 reactive bands was further indicated by control Western blot analysis with an anti-Flag antibody which largely recapitulated what was seen with SAM11. Although N19 signal did not match as closely with the anti-Flag antibody control, support for the specificity of the N19 reactive smear was provided by analysis of DU145 and PC3 prostate cancer cells and cells from Par1 knockout mice reconstituted to express PAR2 (NILF-PAR2 cells) in which PAR2 was detected as a smear that was sensitive to tunicamycin-mediated inhibition of N-glycosylation (Fig. 3). In addition, it is noteworthy that other groups have also reported ectopic PAR2 as appearing as a smear by Western blot analysis. Jacob and colleagues showed that in rat KNRK cells ectopically expressing PAR2, the receptor is detected by anti-Flag Western blot analysis of anti-T7 tag immunoprecipitated material as a smear from ~70–220 kDa (Jacob et al. 2005). This group proposed that the PAR2 smear spanning ~55–110 kDa is likely not ubiquitinated while PAR2 molecular weights above this range is due to mono-ubiquitination of this receptor (Jacob et al. 2005). Another report using an anti-haemagglutinin (HA) tag antibody detected carboxyl terminal HA tagged PAR as a smear ranging from ~55 to ~100 kDa (Compton et al. 2002). This report demonstrated that N-glycosylation at N30 and N222 is a cause of high molecular weight PAR2 as mutagenesis of these sites reduced the PAR2 smear to 33–48 kDa (Compton et al. 2002). Consistently, we have shown that inhibition of N-glycosylation by growth of PC3 cells in the presence of tunicamycin caused the membrane-specific smear detected by antibody N19 to collapse to a band of ~50 kDa, and this was not seen with the SAM11 antibody. Also, similar protein smears have been reported for other GPCRs including

the free fatty acid receptor GPR120 (Miyauchi et al. 2009) and endogenous PAR1 (Russo et al. 2009). Accordingly, while it is clear that our controls ensured that we identified SAM11, C17 and N19 reactivity that was specific for ectopic PAR2, it is not clear why the SAM11 and anti-Flag reactivity differed from that of N19 and C17. A possibility is that the epitopes recognised by the former antibodies are masked when PAR2 is in certain conformations that are not disrupted by denaturing Western blot analysis conditions. This requires further investigation that could include analysis of additional cell fractions and changes in electrophoresis conditions to examine whether this could expose the relevant PAR2 epitopes recognised by the antibodies.

A further appropriate conclusion from our data is that it demonstrates that the Western blot signals in data sheets provided by the supplier for all four antibodies are non-specific and should not be relied upon. In addition, we note that understanding the differences in reactivity of the examined anti-PAR2 antibodies in Western blot, immunocytochemical and flow cytometry analyses is not helped by a lack of disclosure by the supplier of the epitopes used to generate N19 and C17 and the lack of knowledge of the epitope recognised by antibody H99. In addition, while the sequence against which SAM11 was generated is available, we did not consider it appropriate to employ this peptide in preabsorption experiments to attempt to block the specific reactivity of SAM11 as it has recently been demonstrated that this approach is not sufficient to show antibody selectivity (Michel et al. 2009). In particular, a recent series of reports has demonstrated that these blocking peptides can be effective at reducing or eliminating antibody signal without the eliminated reaction representing the target protein (Hamdani and van der Velden 2009; Jositsch et al. 2009).

The examination of endogenous PAR2 in living cells requires antibodies that detect epitopes located on the extracellular side of the plasma membrane. As antibodies SAM11 and N19 are the only anti-PAR2 antibodies that were generated against such epitopes, these were evaluated by flow cytometry. This indicated that while both antibodies are capable of detecting both ectopically and endogenously expressed cell surface located receptor, N19 proved more sensitive than SAM11. Nevertheless, SAM11 has previously been used to evaluate cell surface expression of PAR2 in several cell types including prostate cancer lines (Mize et al. 2008; Ramsay et al. 2008), dendritic cells (Csernok et al. 2006), primary chondrocytes (Ferrell et al. 2010), polymorphonuclear neutrophils following fungi exposure (Moretti et al. 2008) and osteoarthritic osteoblasts compared with non-diseased osteoblasts (Amiable et al. 2009). Recently, anti-PAR2 antibody N19 has been used to follow variations in the level of cell surface receptor following PAR2 agonist treatment in HT29 colon cancer cells (Suen et al. 2012) and also to examine the impact of the post-translational modification palmitoylation on cell surface PAR2 in the prostate cancer cell lines PC3, DU145 and 22Rv1 (Adams et al. 2011a).

Our finding that antibodies N19 and SAM11 specifically detect PAR2 by flow cytometry is consistent with the use of these reagents in other approaches requiring recognition of natively folded and endogenously expressed receptor including immunohistochemical analysis of tissues and assays that require blocking of PAR2 function. In fact, N19 has been used to assess PAR2 expression by immunohistochemistry in the mucosa of experimentally induced colitis in rats (Lohman et al. 2012) as well as its elevated expression in lesional skin from patients with atopic dermatitis (Buddenkotte et al. 2005). Similarly, SAM11 has been used extensively to examine PAR2 expression and localisation in tissues by this technique including in human conjunctival fibroblasts (Asano-Kato et al. 2005) and hepatocellular carcinoma (Kaufmann et al. 2009) as well as in mucosal mast cells in Crohn's ileitis (Christerson et al. 2009), rheumatoid arthritic synovial membranes (Kelso et al. 2006) and prostate cancer bone metastasis lesions (Ramsay et al. 2008). SAM11 has also been used to block PAR2 activation in vivo resulting in protection against both experimental osteoarthritis in a murine model (Ferrell et al. 2010) and carrageenan/kaolin-induced joint inflammation in mice (Kelso et al. 2006). Also, blocking of PAR2 proteolysis with SAM11 prevented protease-mediated allergic sensitisation and airway inflammation (Arizmendi et al. 2011).

In summary, the specificity of four anti-PAR2 antibodies, SAM11, H99, C17 and N19, has been examined. Our data demonstrate that while N19 may be the only antibody suitable for detection of endogenous PAR2 by Western blot analysis, both N19 and SAM11 are suitable for detecting endogenous receptor by flow cytometry. We also found that of the four anti-PAR2 antibodies, three, SAM11, C17 and N19, were able to detect ectopically expressed PAR2 by Western blot and immunocytochemical analysis. Importantly, this study highlights the importance of systematic analysis to assess the specificity of antibodies.

Acknowledgments This work was supported by National Health and Medical Research Council grant #614206 and a Cancer Council Queensland grant (J. D. H.), and an Australian Post-Graduate Award (M. N. A.). We thank Dr Patricia Andrade-Gordon (Johnson & Johnson Pharmaceutical Research and Development, Spring House, PA) for NILF, NILF-PAR1, NILF-PAR2 and NILF-PAR4 cells.

References

Adams MN, Christensen ME, He Y, Waterhouse NJ, Hooper JD (2011a) The role of palmitoylation in signalling, cellular trafficking and plasma membrane localization of protease-activated receptor-2. PLoS One 6:e28018

Adams MN, Ramachandran R, Yau MK, Suen JY, Fairlie DP, Hollenberg MD, Hooper JD (2011b) Structure, function and

pathophysiology of protease activated receptors. Pharmacol Ther 130:248–282

Amiable N, Tat SK, Lajeunesse D, Duval N, Pelletier JP, Martel-Pelletier J, Boileau C (2009) Proteinase-activated receptor (PAR)-2 activation impacts bone resorptive properties of human osteoarthritic subchondral bone osteoblasts. Bone 44:1143–1150

Andrade-Gordon P, Maryanoff BE, Derian CK, Zhang HC, Addo MF, Darrow AL, Eckardt AJ, Hoekstra WJ, McComsey DF, Oksenberg D, Reynolds EE, Santulli RJ, Scarborough RM, Smith CE, White KB (1999) Design, synthesis, and biological characterization of a peptide-mimetic antagonist for a tethered-ligand receptor. Proc Natl Acad Sci U S A 96:12257–12262

Arizmendi NG, Abel M, Mihara K, Davidson C, Polley D, Nadeem A, El Mays T, Gilmore BF, Walker B, Gordon JR, Hollenberg MD, Vliagoftis H (2011) Mucosal allergic sensitization to cockroach allergens is dependent on proteinase activity and proteinase-activated receptor-2 activation. J Immunol 186:3164–3172

Asano-Kato N, Fukagawa K, Okada N, Dogru M, Tsubota K, Fujishima H (2005) Tryptase increases proliferative activity of human conjunctival fibroblasts through protease-activated receptor-2. Invest Ophthalmol Vis Sci 46:4622–4626

Bohm SK, Khitin LM, Grady EF, Aponte G, Payan DG, Bunnett NW (1996) Mechanisms of desensitization and resensitization of proteinase-activated receptor-2. J Biol Chem 271:22003–22016

Buddenkotte J, Stroh C, Engels IH, Moormann C, Shpacovitch VM, Seeliger S, Vergnolle N, Vestweber D, Luger TA, Schulze-Osthoff K, Steinhoff M (2005) Agonists of proteinase-activated receptor-2 stimulate upregulation of intercellular cell adhesion molecule-1 in primary human keratinocytes via activation of NF-kappa B. J Invest Dermatol 124:38–45

Camerer E, Huang W, Coughlin SR (2000) Tissue factor- and factor X-dependent activation of protease-activated receptor 2 by factor VIIa. Proc Natl Acad Sci USA 97:5255–5260

Christerson U, Keita AV, Soderholm JD, Gustafson-Svard C (2009) Increased expression of protease-activated receptor-2 in mucosal mast cells in Crohn's ileitis. J Crohns Colitis 3:100–108

Compton SJ, Sandhu S, Wijesuriya SJ, Hollenberg MD (2002) Glycosylation of human proteinase-activated receptor-2 (hPAR2): role in cell surface expression and signalling. Biochem J 368:495–505

Csernok E, Ai M, Gross WL, Wicklein D, Petersen A, Lindner B, Lamprecht P, Holle JU, Hellmich B (2006) Wegener autoantigen induces maturation of dendritic cells and licenses them for Th1 priming via the protease-activated receptor-2 pathway. Blood 107:4440–4448

Dery O, Thoma MS, Wong H, Grady EF, Bunnett NW (1999) Trafficking of proteinase-activated receptor-2 and beta-arrestin-1 tagged with green fluorescent protein. Beta-Arrestin-dependent endocytosis of a proteinase receptor. J Biol Chem 274:18524–18535

Ferrell WR, Kelso EB, Lockhart JC, Plevin R, McInnes IB (2010) Protease-activated receptor 2: a novel pathogenic pathway in a murine model of osteoarthritis. Ann Rheum Dis 69:2051–2054

Georgy SR, Pagel CN, Wong DM, Sivagurunathan S, Loh LH, Myers DE, Hollenberg MD, Pike RN, Mackie EJ (2010) Proteinase-activated receptor-2 (PAR2) and mouse osteoblasts: regulation of cell function and lack of specificity of PAR2-activating peptides. Clin Exp Pharmacol Physiol 37:328–336

Georgy SR, Pagel CN, Ghasem-Zadeh A, Zebaze RM, Pike RN, Sims NA, Mackie EJ (2011) Proteinase-activated receptor-2 is required for normal osteoblast and osteoclast differentiation during skeletal growth and repair. Bone 50:704–712

Hamdani N, van der Velden J (2009) Lack of specificity of antibodies directed against human beta-adrenergic receptors. Naunyn Schmiedebergs Arch Pharmacol 379:403–407

He Y, Wortmann A, Burke LJ, Reid JC, Adams MN, Abdul-Jabbar I, Quigley JP, Leduc R, Kirchhofer D, Hooper JD (2010) Proteolysis-induced N-terminal ectodomain shedding of the integral membrane glycoprotein CUB domain-containing protein 1 (CDCP1) is accompanied by tyrosine phosphorylation of its C-terminal domain and recruitment of Src and PKCδ. J Biol Chem 285:26162–26173

Hooper JD, Zijlstra A, Aimes RT, Liang H, Claassen GF, Tarin D, Testa JE, Quigley JP (2003) Subtractive immunization using highly metastatic human tumor cells identifies SIMA135/CDCP1, a 135 kDa cell surface phosphorylated glycoprotein antigen. Oncogene 22:1783–1794

Ishihara H, Connolly AJ, Zeng D, Kahn ML, Zheng YW, Timmons C, Tram T, Coughlin SR (1997) Protease-activated receptor 3 is a second thrombin receptor in humans. Nature 386:502–506

Jacob C, Cottrell GS, Gehringer D, Schmidlin F, Grady EF, Bunnett NW (2005) c-Cbl mediates ubiquitination, degradation, and down-regulation of human protease-activated receptor 2. J Biol Chem 280:16076–16087

Jositsch G, Papadakis T, Haberberger RV, Wolff M, Wess J, Kummer W (2009) Suitability of muscarinic acetylcholine receptor antibodies for immunohistochemistry evaluated on tissue sections of receptor gene-deficient mice. Naunyn Schmiedebergs Arch Pharmacol 379:389–395

Kagota S, Chia E, McGuire JJ (2011) Preserved arterial vasodilatation via endothelial protease-activated receptor-2 in obese type 2 diabetic mice. Br J Pharmacol 164:358–71

Kaufmann R, Oettel C, Horn A, Halbhuber KJ, Eitner A, Krieg R, Katenkamp K, Henklein P, Westermann M, Bohmer FD, Ramachandran R, Saifeddine M, Hollenberg MD, Settmacher U (2009) Met receptor tyrosine kinase transactivation is involved in proteinase-activated receptor-2-mediated hepatocellular carcinoma cell invasion. Carcinogenesis 30:1487–1496

Kaushal A, Myers SA, Dong Y, Lai J, Tan OL, Bui LT, Hunt ML, Digby MR, Samaratunga H, Gardiner RA, Clements JA, Hooper JD (2008) A novel transcript from the KLKP1 gene is androgen regulated, down-regulated during prostate cancer progression and encodes the first non-serine protease identified from the human kallikrein gene locus. Prostate 68:381–399

Kelso EB, Lockhart JC, Hembrough T, Dunning L, Plevin R, Hollenberg MD, Sommerhoff CP, McLean JS, Ferrell WR (2006) Therapeutic promise of proteinase-activated receptor-2 antagonism in joint inflammation. J Pharmacol Exp Ther 316:1017–1024

Lohman RJ, Cotterell AJ, Suen J, Liu L, Do AT, Vesey DA, Fairlie DP (2012) Antagonism of protease-activated receptor 2 protects against experimental colitis. J Pharmacol Exp Ther 340(2):256–265

Macfarlane SR, Seatter MJ, Kanke T, Hunter GD, Plevin R (2001) Proteinase-activated receptors. Pharmacol Rev 53:245–282

Michel MC, Wieland T, Tsujimoto G (2009) How reliable are G-protein-coupled receptor antibodies? Naunyn Schmiedebergs Arch Pharmacol 379:385–388

Miyauchi S, Hirasawa A, Iga T, Liu N, Itsubo C, Sadakane K, Hara T, Tsujimoto G (2009) Distribution and regulation of protein expression of the free fatty acid receptor GPR120. Naunyn Schmiedebergs Arch Pharmacol 379:427–434

Mize GJ, Wang W, Takayama TK (2008) Prostate-specific kallikreins-2 and -4 enhance the proliferation of DU-145 prostate cancer cells through protease-activated receptors-1 and -2. Mol Cancer Res 6:1043–1051

Molino M, Barnathan ES, Numerof R, Clark J, Dreyer M, Cumashi A, Hoxie JA, Schechter N, Woolkalis M, Brass LF (1997) Interactions of mast cell tryptase with thrombin receptors and PAR-2. J Biol Chem 272:4043–4049

Moretti S, Bellocchio S, Bonifazi P, Bozza S, Zelante T, Bistoni F, Romani L (2008) The contribution of PARs to inflammation and immunity to fungi. Mucosal Immunol 1:156–168

Nystedt S, Emilsson K, Wahlestedt C, Sundelin J (1994) Molecular cloning of a potential proteinase activated receptor. Proc Natl Acad Sci U S A 91:9208–9212

Nystedt S, Emilsson K, Larsson AK, Strombeck B, Sundelin J (1995) Molecular cloning and functional expression of the gene encoding the human proteinase-activated receptor 2. Eur J Biochem 232:84–89

Oikonomopoulou K, Hansen KK, Saifeddine M, Tea I, Blaber M, Blaber SI, Scarisbrick I, Andrade-Gordon P, Cottrell GS, Bunnett NW, Diamandis EP, Hollenberg MD (2006) Proteinase-activated receptors, targets for kallikrein signaling. J Biol Chem 281:32095–32112

Ramachandran R, Noorbakhsh F, Defea K, Hollenberg MD (2012) Targeting proteinase-activated receptors: therapeutic potential and challenges. Nat Rev Drug Disc 11:69–86

Ramsay AJ, Dong Y, Hunt ML, Linn M, Samaratunga H, Clements JA, Hooper JD (2008) Kallikrein-related peptidase 4 (KLK4) initiates intracellular signaling via protease-activated receptors (PARs). KLK4 and PAR-2 are co-expressed during prostate cancer progression. J Biol Chem 283:12293–12304

Ricks TK, Trejo J (2009) Phosphorylation of protease-activated receptor-2 differentially regulates desensitization and internalization. J Biol Chem 284:34444–34457

Roosterman D, Schmidlin F, Bunnett NW (2003) Rab5a and rab11a mediate agonist-induced trafficking of protease-activated receptor 2. Am J Physiol 284:C1319–1329

Russo A, Soh UJ, Paing MM, Arora P, Trejo J (2009) Caveolae are required for protease-selective signaling by protease-activated receptor-1. Proc Natl Acad Sci U S A 106:6393–6397

Suen JY, Barry GD, Lohman RJ, Halili MA, Cotterell AJ, Le GT, Fairlie DP (2012) Modulating human proteinase activated receptor 2 with a novel antagonist (GB88) and agonist (GB110). Br J Pharmacol 165:1413–1423

Vu TK, Hung DT, Wheaton VI, Coughlin SR (1991) Molecular cloning of a functional thrombin receptor reveals a novel proteolytic mechanism of receptor activation. Cell 64:1057–1068

Wortmann A, He Y, Deryugina EI, Quigley JP, Hooper JD (2009) The cell surface glycoprotein CDCP1 in cancer–insights, opportunities, and challenges. IUBMB life 61:723–730

Xu WF, Andersen H, Whitmore TE, Presnell SR, Yee DP, Ching A, Gilbert T, Davie EW, Foster DC (1998) Cloning and characterization of human protease-activated receptor 4. Proc Natl Acad Sci USA 95:6642–6646